Multiphase semiclassical approximation of the one-dimensional harmonic crystal: I. The periodic case

2006 J. Phys. A: Math. Gen. 39 10509

(http://iopscience.iop.org/0305-4470/39/33/018)

INSTITUTE OF PHYSICS PUBLISHING JOURNAL OF PHYSICS A: MATHEMATICAL AND GENERAL

J. Phys. A: Math. Gen. **39** (2006) 10509–10521 doi:10.1088/0305-4470/39/33/018

Multiphase semiclassical approximation of the one-dimensional harmonic crystal: I. The periodic case

Laurent Gosse

Istituto per le Applicazioni del Calcolo (sezione di Bari), via G. Amendola, 122/D, 70126 Bari, Italy

E-mail: l.gosse@ba.iac.cnr.it

Received 12 December 2005, in final form 16 June 2006
Published 2 August 2006
Online at stacks.iop.org/JPhysA/39/10509

Abstract

One-dimensional electronic conduction is investigated in a special case usually referred to as the harmonic crystal, meaning essentially that atoms are assumed to move like coupled harmonic oscillators within the Born–Oppenheimer approximation. We recall their dispersion relation and derive a WKB system approximately satisfied by any electron's wavefunction inside a given energy band. This is then numerically solved according to the method of K-branch solutions. Numerical results are presented in the case where atoms move with one- or two-modes vibrations; finally, we include the case where the Poisson self-interaction potential also influences the electrons' dynamics.

PACS numbers: 03.65.Sq, 02.30.Jr
Mathematics Subject Classification: 81Q05, 81Q20, 35L65, 65M06

(Some figures in this article are in colour only in the electronic version)

1. Introduction

1.1. Preliminaries

It is a familiar fact that electrons are able to move over long distances inside certain materials; this phenomenon manifests itself, for instance, through the high electrical conductivity of metals. However, even in the purest metals, electrons are influenced by the underlying lattice made of the atoms constituting the crystal itself. A very reasonable assumption is to consider the repartition of these atoms as periodic; such an idealization allows us to take advantage of Bloch's theory which explains how valence/conduction electrons can move rather freely and have a well-defined (Bloch) momentum. Indeed, Bloch's theorem is one example of coherent electronic transport: in a perfect crystal at zero temperature, there is a great superposition of

phase-coherent waves with similar wavenumbers which results in a frictionless flow inside the material (at low densities, Pauli's exclusion principle does not have very sensible effects). These electrons move according to the energy bands thus can survive multiple scattering events with the atoms without getting localized and accumulating somewhere. Unfortunately, finite conductivity is observed in practice because no sample will be pure enough to be a perfectly periodic lattice, and even if this idealization was realizable, vibrations due to thermal excitation would perturb the picture. The effects of these vibrations constitute the main point we want to study in this paper within a simplified framework.

We are interested in deriving approximate WKB solutions of certain Schrödinger equations in one space dimension, where short-range scattering effects other than those considered in the Bloch decomposition will be neglected. In other words, we shall work on ballistic transport of electrons for which the most important long-range interaction is the Coulomb force. In case one assumes translational invariance in two directions, three-dimensional objects can be modelled to some extent by means of a one-dimensional equation. We shall follow these ideas which have already been studied in former works [9–11]. However, we now go one step further considering that atoms vibrate as 'coupled harmonic oscillators'. The Hamiltonian for one electron reads (see [1], p 430), with obvious notation,

$$\mathcal{H}_{\text{full}} = \frac{p^2}{2m} + \sum_{\alpha\in\mathbb{Z}} \frac{P_\alpha^2}{2M} + \sum_{\alpha\in\mathbb{Z}} V_{\text{ions}}(|X_\alpha - X_{\alpha-1}|) + \sum_{\alpha\in\mathbb{Z}} V_{\text{ion}-e^-}(|x - X_\alpha|). \quad (1)$$

Parameters (p, x, m) refer to some electron and $(P_\alpha, X_\alpha, M)_\alpha$ to the collection of atomic cores. One could also consider a cloud of electrons indexed by $\beta \in \mathbb{Z}$ and the first term in (1) should be replaced by

$$\sum_{\beta\in\mathbb{Z}} \frac{p_\beta^2}{2m} + \frac{1}{2} \sum_{\beta\neq\beta'} \frac{e^2}{|x_\beta - x_{\beta'}|}.$$

Then Coulomb self-interactions may be treated via 'mean-field', which would lead to some Hartree equation, cf [11]; this will be briefly considered in the numerical results of section 4.3. But first, let us concentrate on the one-particle model (1). We shall assume the following hypotheses to hold throughout the whole paper:

- ionic cores are coupled oscillators, i.e. $V_{\text{ions}}(|X_\alpha - X_{\alpha-1}|) = \frac{1}{2}M\omega^2(X_\alpha - X_{\alpha-1})^2$;
- they are treated classically (Born–Oppenheimer approximation) because $\frac{m}{M} \ll 1$;
- they influence electrons but not the opposite (there are no polarons, cf [1, 18]).

1.2. Modelling of ionic cores' vibrations

Without V_{ions}, ions would arrange periodically $\bar{X}_\alpha = 2\pi\alpha, \alpha \in \mathbb{Z}$, as in [9]; now, let us call $U_\alpha(t) := X_\alpha(t) - 2\pi\alpha$ the displacement around these abscissae 'at rest'. The cores' equation is decoupled thanks to our third hypothesis:

$$\frac{\mathrm{d}}{\mathrm{d}t^2} U_\alpha(t) - \omega^2(U_{\alpha+1}(t) - 2U_\alpha(t) + U_{\alpha-1}(t)) = 0.$$

As for the continuous wave equation, it can be solved by Fourier series:

$$Q(t,k) = \sum_{\alpha\in\mathbb{Z}} U_\alpha(t) \exp(-\mathrm{i}k2\pi\alpha) \Rightarrow \frac{\mathrm{d}}{\mathrm{d}t^2} Q(t,k) = \Omega(k)^2 Q(t,k).$$

The dispersion relation reads (see also [1])

$$\Omega(k) = 2\omega|\sin(k\pi)|, \qquad k \in \mathcal{B} := \left]-\frac{1}{2}, \frac{1}{2}\right[,$$

with $\mathcal{B}$ being the Brillouin zone associated with the Bravais lattice for the ionic cores 'at rest'. $U_\alpha(t)$ can be written as a continuous summation of plane waves:

$$U_\alpha(t) = \int_0^{\frac{1}{2}} A(k)\exp(\mathrm{i}(k2\pi\alpha - \Omega(k)t)) + B(k)\exp(-\mathrm{i}(k2\pi\alpha - \Omega(k)t)).\mathrm{d}k. \tag{2}$$

The Schrödinger equation for the electron's wavefunction ψ becomes accordingly,

$$\mathrm{i}\hbar\partial_t\psi + \frac{\hbar^2}{2m}\partial_{xx}\psi = V_{\mathrm{per}}(x + U_\alpha(\varepsilon t))\psi, \tag{3}$$

with $V_{\mathrm{per}}(x) \simeq \sum_\alpha V_{\mathrm{ion}-e^-}(|x - \bar{X}_\alpha|)$, which can be considered 2π-periodic and smooth; the dimensionless parameter $\varepsilon = \bar{T}_{e^-}/\bar{T}_{\mathrm{ions}}$ is defined as the ratio of characteristic times for the movements of ions and electrons, respectively. This modelling has already been encountered in several papers; let us quote [19, 22] where it is referred to as 'the deformed crystal'. Moreover, many studies have been made in the field of 'incommensurate crystals', see [15, 17, 20], emphasizing the so-called modulated Kronig–Penney model. This is somewhat an extreme case for which the potential given in (3) is no longer periodic thus the Brillouin zone of the resulting crystal is reduced to a point. We believe that new methods are needed for tackling such a problem of non-periodic homogenization which goes beyond the scope of the present paper. Indeed, the present text deals only with perturbed potentials (as shown on the right-hand side of (3)) endowed with some periodicity in the x variable.

2. WKB asymptotic expansions of wavefunctions

We assume the reader to be familiar with Bloch's theory; a comprehensive presentation is given in [1], see also [6, 7, 9, 13, 14]. In this section, we shall show that for simple enough displacements (2) (typically with few vibration modes), it is possible to derive a WKB approximation for the wavefunction ψ solution of (3) for smooth V_{per}. For simplicity, we switch at once to 'atomic units' for which $\hbar = m = e = 1$ and seek a convenient ansatz as variables are rescaled according to $(t, x) \to (\varepsilon t, \varepsilon x)$ with $0 < \varepsilon \ll 1$; $\varepsilon = 0$ would mean that phonon scattering acts instantaneously.

2.1. Bloch theory and the Eikonal equation

We are now basically interested in the following equation:

$$\mathrm{i}\varepsilon\partial_t\psi + \frac{\varepsilon^2}{2}\partial_{xx}\psi = \tilde{V}_{\mathrm{per}}\left(t, \frac{x}{\varepsilon}\right)\psi, \qquad \tilde{V}_{\mathrm{per}}(t, y) = V_{\mathrm{per}}(y + u(t, y)), \tag{4}$$

where $y = x/\varepsilon$ is the microscopic variable, $\tilde{V}_{\mathrm{per}}$ is supposed to be C^∞ in both variables, the motion u is smooth and periodic in both its variables and V_{per} is 2π-periodic. The simplest case where u is only endowed with a unique vibration mode is displayed in figure 1. Let us assume that for all t, $\tilde{V}_{\mathrm{per}}(t, y) + 2\pi/k = V_{\mathrm{per}}(t, y)$; thus one can consider a slightly generalized Bloch eigenvalue problem:

$$\forall t \in \mathbb{R}, \qquad -\tfrac{1}{2}\partial_{yy}\Psi_{n,\kappa}(t, y) + \tilde{V}_{\mathrm{per}}(t, y)\Psi_{n,\kappa}(t, y) = E_n(t, \kappa)\Psi_{n,\kappa}(t, y), \tag{5}$$

for any $t \in \mathbb{R}^+$ and $\Psi_{n,\kappa}(t, y) = \exp(i\kappa y)z_{n,\kappa}(t, y)$ a Bloch state. We observe that we only need $y \in]0, 2\pi/k[$ and the Brillouin zone corresponding to $\tilde{V}_{\mathrm{per}}$ is smaller than $\mathcal{B}$,

$$\kappa \in \tilde{\mathcal{B}} = \left]-\frac{k}{2}, \frac{k}{2}\right[, \qquad |k| \leqslant \frac{1}{2}.$$

Since there is no differentiation in time inside (5), standard results remain valid (see e.g. [16]) and ensure that for any fixed t and $\kappa \in \tilde{\mathcal{B}}$, there exists a complete set of eigenfunctions

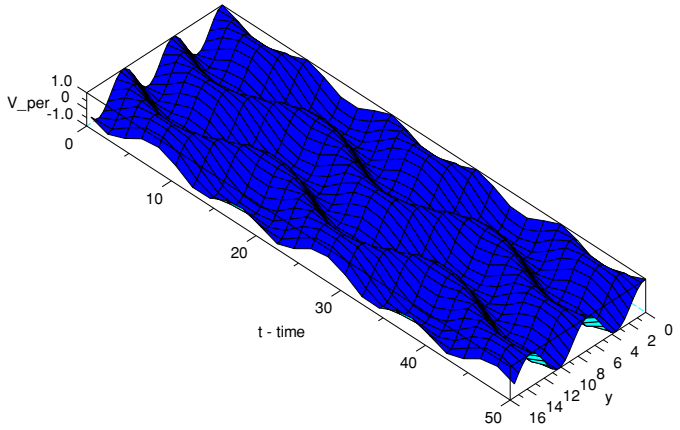

Figure 1. Time evolution for periodic potential in (4) with $V_{\rm per}(y) = \cos(y)$ and $u(t, y) = \sin(ky + \Omega(k)t)$, $k \simeq 0.02$, $\varepsilon = 1$.

$\Psi_{n,\kappa}(t, .) \in L^2(0, 2\pi/k)$ with countably many eigenvalues $E_1(t, \kappa) < E_2(t, \kappa) < \cdots < E_{n-1}(t, \kappa) < E_n(t, \kappa) < \cdots$ depending smoothly on time. The set $\{E_n(t, \kappa); \kappa \in \tilde{\mathcal{B}}\}$ is called the nth energy band whereas $\Psi_{n,\kappa}$ is an nth Bloch state having the form $\exp(\mathrm{i}\kappa y) z_{n,\kappa}(t, y)$ for a certain $2\pi/k$-periodic modulation. Modulations can be normalized so as to form an orthonormal base of $L^2(0, 2\pi/k)$ for each $t > 0$.

At this level, we introduce a WKB ansatz for ψ considering a two-scale amplitude:

$$A\left(t, x, y = \frac{x}{\varepsilon}\right) = A_0(t, x, y) + \varepsilon A_1(t, x, y) + \cdots; \qquad A(t, x, y + 2\pi/k) = A(t, x, y). \tag{6}$$

Plugging the approximation $A(t, x, x/\varepsilon)\exp(i\varphi(t, x)/\varepsilon)$ inside (4) and balancing the $O(1)$ terms following carefully [6, 7, 13] can be shown to lead to a Hamilton–Jacobi equation for the phase

$$\partial_t \varphi + E_n(t, \partial_x \varphi) = 0. \tag{7}$$

2.2. *Derivation of the transport equation*

The principal amplitude stems from balancing $O(\varepsilon)$ terms and is usually handled by means of the 'Feshbach method'; see the paper [6] to which we refer for a detailed presentation of the computation. Here we shall limit ourselves to specify the changes occurring in the derivation because of the time dependence of $\tilde{V}_{\rm per}$. Actually, everything proceeds as in appendix A of [6], except for the last step that we explain now[1]: let us denote $\mathcal{L}$ the usual geometric optics transport operator associated with the Bloch theory:

$$\mathcal{L}a := E_n'(t, \partial_x\varphi)\partial_x a + \tfrac{1}{2}\partial_x(E_n'(t, \partial_x\varphi))a,$$

where E_n' stands for the partial derivative with respect to κ. The principal amplitude is defined as $a_0(t, x)$ such that there holds $A_0(t, x, y) = a_0(t, x) z_{n,\kappa}(t, y)$, for $\kappa = \partial_x\varphi(t, x)$. From (A.4)–(A.6) in [6], we obtain the following equation for a_0:

$$\partial_t a_0 + a_0 \int_0^{2\pi/k} g_n \overline{\partial_t g_n}.\mathrm{d}y + E_n'(t, \partial_x\varphi)a_0 \int_0^{2\pi/k} g_n \overline{\partial_x g_n}.\mathrm{d}y + \mathcal{L}a_0 = 0, \tag{8}$$

[1] We shall use the same notations for easiness in reading.

where $g_n(t,x,y) = z_{n,\kappa=\partial_x\varphi(t,x)}(t,y)$ and $\bar{\cdot}$ stands for complex conjugation. Now, as a consequence of the modulation's normalization, $\|z_{n,\kappa}(t,.)\|_{L^2(0,2\pi/k)} = 1$, we observe that the first coefficient acting on a_0 is purely imaginary,

$$\partial_t \int_0^{2\pi/k} g_n\overline{g_n}.\mathrm{d}y = 0 = 2\,\mathrm{Re}\left(\int_0^{2\pi/k} g_n\overline{\partial_t g_n}.\mathrm{d}y\right),$$

and since $E_n' \in \mathbb{R}$, the next one as well. It remains to make use of the definition of g_n, the chain rule, and equation (7) to compute

$$\int_0^{2\pi/k} g_n\{\overline{\partial_t g_n + E_n'(t,\partial_x\varphi)\partial_x g_n}\}.\mathrm{d}y = \int_0^{2\pi/k} z_{n,\partial_x\varphi(t,x)}\ \overline{\partial_t z_{n,\kappa}}\big|_{\kappa=\partial_x\varphi(t,x)}.\mathrm{d}y.$$

We denote this term $\beta(t,x) \in \mathrm{i}\mathbb{R}$; it identifies with a Berry phase [3], and stems from the time dependence of the Bloch states. In case another slowly varying potential $V(t,x)\psi$ is added on the right-hand side of (4), one would get another phase shift too reading $\partial_x V(t,x)\int_0^{2\pi/k} z_{n,\partial_x\varphi(t,x)}\ \overline{\partial_\kappa z_{n,\kappa}}\big|_{\kappa=\partial_x\varphi(t,x)}.\mathrm{d}y \in \mathrm{i}\mathbb{R}$ as in [6, 7, 10]. Anyway, it now remains to multiply the resulting equation (8) by $\bar{a}_0$ and take its real part to derive the usual continuity equation for $|a_0|^2$:

$$\partial_t|a_0|^2 + \partial_x(E_n'(t,\partial_x\varphi)|a_0|^2) = 0. \tag{9}$$

All in all, we have shown that an approximate nth band solution for (4) reads

$$\psi^\varepsilon(t,x) = a_0(t,x)\exp(\mathrm{i}\varphi(t,x)/\varepsilon)z_{n,\partial_x\varphi(t,x)}(t,x/\varepsilon), \qquad t \geqslant 0, \tag{10}$$

and evolves in time according to the WKB system made of (7) and (9). A first consequence is that an initial datum concentrated on a given band will necessarily give rise to an approximate solution in the same band. Lattice vibrations are not supposed to make electrons' trigger interband transitions; hence from now on, we consider some electron moving according to some energy band whose index $n \in \mathbb{N}$ is fixed.

2.3. 'Lattice tracking' phenomenon

Clearly, each primitive cell of the 'perturbed lattice' contains $\frac{1}{|k|} \in \mathbb{N}$ atomic cores. We modified the algorithm in [10], section 2.2 in order to compute numerically $E_n(t,\kappa)$, $\Psi_{n,\kappa}(t,y)$ by means of a spectral method. We write

$$\Psi_{n,\kappa}(t,y) = \sum_{\ell\in\mathbb{Z}} \hat{\Psi}^\ell_{n,\kappa}(t)\exp(i(\kappa+k\ell)y), \qquad \hat{\Psi}^\ell_{n,\kappa}(t) = \int_0^{2\pi/k} z_{n,\kappa}(t,y)\exp(-i\ell y).\mathrm{d}y.$$

The same decomposition is carried out for the perturbed potential and one is led to diagonalize a matrix H_κ similar to that in [10] with kinetic energy terms reading now $\frac{1}{2}(\kappa+k\ell)^2$, $\ell = -N,\ldots,N$. Modulations $z_{n,\kappa}$ are recovered by fast Fourier transform (`fft`) of corresponding eigenvectors and they hold for some $t \in \mathbb{R}^+$, $n \in \mathbb{N}$:

$$E_n(t,\kappa) = \frac{\hat{E}_0(t)}{2} + \sum_{q\in\mathbb{N}^*} \hat{E}_q(t)\cos(2\pi q\kappa/k), \qquad \hat{E}_q(t) = 4\int_0^{\frac{k}{2}} E_n(t,\kappa)\cos(2\pi q\kappa/k).\mathrm{d}\kappa.$$

Since there are $1/k$ atoms per period, bands 'stick together' and constitute clusters of $1/k$ (for k small, there would be 'bands of bands' emerging inside a tiny Brillouin zone). In the ground state, each of the $1/k$ modulations is peaked around the corresponding atom in the elementary cell: see figure 2 where $\tilde{V}_{\mathrm{per}}(t,y) = \cos\left(y + \frac{\pi}{2}\sin(ky+\Omega(k)t)\right)$. It is interesting to make a link with a feature pointed out in [22], namely the tendency for the lattice to drag the electron with its displacement motion, called 'lattice tracking'. First, observe that even if supplying

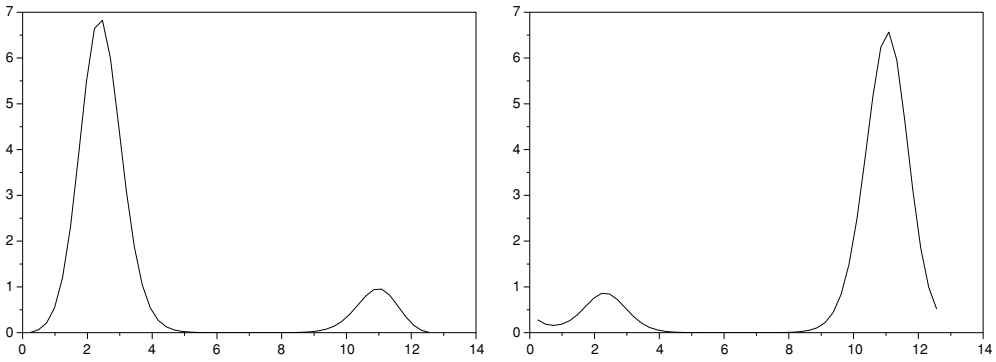

Figure 2. Two lowest modulations $|z_{n,\kappa=0}|^2$ for $k = 0.5$ and $t = 0.1$.

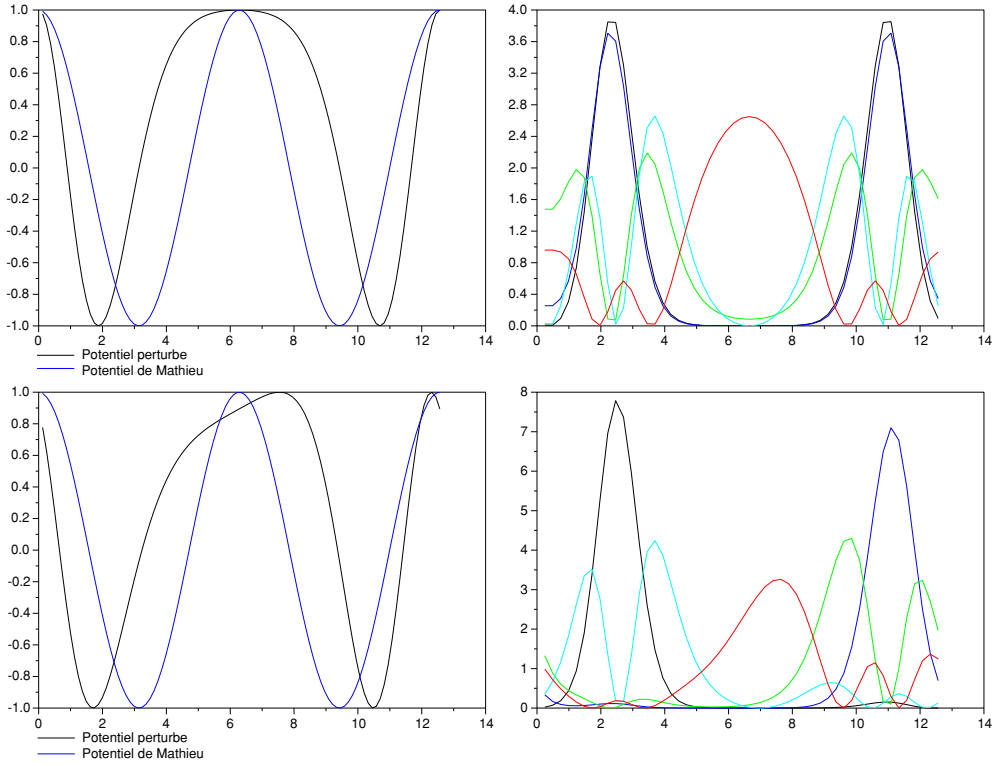

Figure 3. Potentials (left) and lowest modulations $|z_{n,\kappa=0}|^2$ (right) for $t = 0, 0.3$.

the WKB system (7)–(9) with initial data such that $a_0 \equiv 1$ and $\partial_x \varphi \equiv 0$, we would have $|\psi^\varepsilon(t,x)|^2 \neq |\psi^\varepsilon(t=0,x)|^2$ because of the time dependence of $z_{n,\kappa}$. In other words, a small current is created from the motion of the atoms even if the macroscopic quantities remain constant in time. In figure 3, we displayed the deformations of the five lowest modulations with respect to the changes in the same potential $\tilde{V}_{\text{per}}$ as in figure 2. According to [9], section 3.2, this implies the dragging effect suggested in [22].

3. Numerical approximation with *K*-branch solutions

This method has been originally introduced in [8, 21] following the seminal work by Brenier and Corrias [5]. It is based on the remark that geometrical solutions to (7)–(9) can be recovered by solving a rather simple system of nonlinear conservation laws through the moment closure of a kinetic equation. This opens the way of using all the results from the numerical analysis of this kind of problems instead of using the classical Lagrangian framework of ray-tracing algorithms, which may ask for repetitive regridding procedures. Let us also note that the inclusion of the Poisson self-consistent potential would not be easy within a ray-tracing approach.

We do not plan to recall it completely; instead we refer to [9, 10] where it has been explained how to extend it to the case where semi-classical dynamics are driven by energy bands numerically obtained from Bloch's decomposition. The inclusion of the Poisson term for systems endowed with translational invariance in two directions has been described in [11] and will be used in section 4.3. Here we just explain how to handle the time dependence of the energy bands in the processing of the WKB system (7)–(9).

3.1. General procedure

It has been observed [4] that the geometric solutions of scalar conservation laws with a flux $E_n'(.,u) \geqslant 0$ can be recovered out of a kinetic problem,

$$\partial_t f + E_n'(t,\xi)\partial_x f = 0, \qquad f(t=0,x,\xi) = H(u(t=0,x)-\xi)H(\xi),$$

with H being the Heaviside function. Beyond breakup time, the form of f must express the fact that several particles with different velocities can cross each other at the same point x. Thus a more correct representation would be

$$f(t,x,\xi) = \sum_{j=1}^{K} (-1)^{j-1} H(u_j(t,x)-\xi), \tag{11}$$

as long as no more than K-folds appear. A remarkable feature is that (11) can be obtained from an entropy minimization process; this eventually led to the definition of *K-multivalued solutions* in [5].

Definition 1. *We call K-multivalued solution any measurable function $f(t,x,\xi) \in \{0,1\}$ on $\mathbb{R}\times\mathbb{R}^+\times\mathbb{R}^+$ satisfying the following equation in the sense of distributions*

$$\partial_t f + E_n'(t,\xi)\partial_x f = (-1)^{K-1}\partial_\xi^K \mu, \qquad f(t,x,\xi) = \sum_{j=1}^{K}(-1)^{j-1}H(u_j(t,x)-\xi), \tag{12}$$

where μ is a nonnegative Radon measure on $\mathbb{R}\times\mathbb{R}^+\times\mathbb{R}^+$ and $K\in\mathbb{N}$ is given.

The set of $u_j(t,x)$'s is called the *K-branch entropy solution*; as usual, moments $m_i(t,x) = \frac{1}{i}\sum_{j=1}^{K}(-1)^{j-1}u_j(t,x)^{i-1}$, $i = 1,2,\ldots,K$ can be computed, for which an equivalence result holds.

Theorem 1. *(Brenier and Corrias [5]). A measurable function $f(t,x,\xi) = \sum_{j=1}^{K}(-1)^{j-1}H(u_j(t,x)-\xi)$ is a K-multivalued solution if and only if all the following entropy inequalities hold for any θ, $\partial_\xi^K\theta \geqslant 0$:*

$$\partial_t \int_{\mathbb{R}^+}\theta(\xi)f(t,x,\xi).\mathrm{d}\xi + \partial_x\int_{\mathbb{R}^+}E_n'(t,\xi)\theta(\xi)f(t,x,\xi).\mathrm{d}\xi \leqslant 0. \tag{13}$$

Equality holds in case $\partial_\xi^K\theta\equiv 0$, especially for $\theta(\xi)=\xi^j$, $j=0,1,\ldots,K-1$.

We close this section mentioning that the map $\mathbb{R}^K \ni \vec{m} \mapsto \vec{u}$ is called the 'finite Markov moment problem'; this delicate inversion has been recently tackled in [12].

3.2. Moment systems and intensity recovery

Using `fft` routines in 2D (t and κ or y), it is possible to obtain numerically good approximations of the following periodic functions ($T_{\rm per} < +\infty$):

$$[0, T_{\rm per}] \times \tilde{\mathcal{B}} \ni t, \kappa \mapsto E_n(t, \kappa),$$

and,

$$[0, T_{\rm per}] \times \left[0, \frac{2\pi}{k}\right] \times \tilde{\mathcal{B}} \ni t, y, \kappa \mapsto z_{n,\kappa}(t, y).$$

The fact that we restricted ourselves to commensurate crystals is fundamental here. These two representations would not hold in Fourier space without assuming that $\tilde{V}_{\rm per}$ is periodic in both its variables. This leads to restrictions on k's allowed to show up in (2). If one introduces a velocity variable $u = \partial_x \varphi$ in (7), then a scalar conservation law with a time-dependent flux appears,

$$\partial_t u + \partial_x E_n(t, u) = 0, \qquad u(t = 0, .) = \partial_x \varphi(t = 0, .),$$

for which the multivalued (or geometric) solution is to be sought according to the moment system (13). As soon as one completes this programme, the principal intensity $|a_0|^2$ can be easily recovered; indeed, at any time $t > 0$, one deduces from (9) that

$$|a_0|^2(t, x) = |a_0|^2(t = 0, x_0) \left|\frac{\partial x_0}{\partial x}\right|,$$

and from (7) that $x = x_0 + \int_0^t E_n'(s, u(t = 0, x_0)).\mathrm{d}s = x_0 + \int_0^t E_n'(s, u(t, x)).\mathrm{d}s$ with $u(t, x)$ obtained by solving (13). In the homogeneous case, the most accurate way to derive the intensity follows from

$$\left|\frac{\partial x_0}{\partial x}\right| = \left|\frac{\partial x}{\partial x_0}\right|^{-1} = \left|\frac{1}{1 + \partial_x u(t = 0, x_0) \int_0^t E_n''(s, u(t, x)).\mathrm{d}s}\right|,$$

which leads to the expression

$$a_0(t, x) = \frac{a_0(t = 0, x_0)}{\sqrt{\left|1 + \partial_x u(t = 0, x_0) \int_0^t E_n''(s, u(t, x)).\mathrm{d}s\right|}}, \qquad x_0 = x - \int_0^t E_n'(s, u(t, x)).\mathrm{d}s.$$

4. Numerical results

We now aim to show results of K-branch solutions in the context of simple phonon scattering via the WKB approach (7)–(9) and to compare them to direct computations of solutions to (4) using the time-splitting Fourier schemes proposed in [2]. We shall try to show that the smaller the ε, the closer the solutions' observables become. However, only weak convergence of observables can generally be hoped for [16], hence we shall look at the $L^1(\mathbb{R})$ norm of the antiderivative of the difference between position densities:

$$x \mapsto \int_0^x \left(\varrho^{\varepsilon}_{\rm WKB}(T, s) - |\psi(T, s)|^2\right).\mathrm{d}s, \qquad T \in \mathbb{R}^+. \tag{14}$$

This function can be expected to flatten as ε is decreased. $\varrho^{\varepsilon}_{\rm WKB}$ stands for the position density obtained from the WKB ansatz (10). It has been sometimes necessary to filter numerically the Fourier schemes; here we used a standard convolution recipe involving a Gaussian kernel $\exp(-a\xi^2)$, $a \in \mathbb{R}^+$. 512 discretization points have been used for both algorithms.

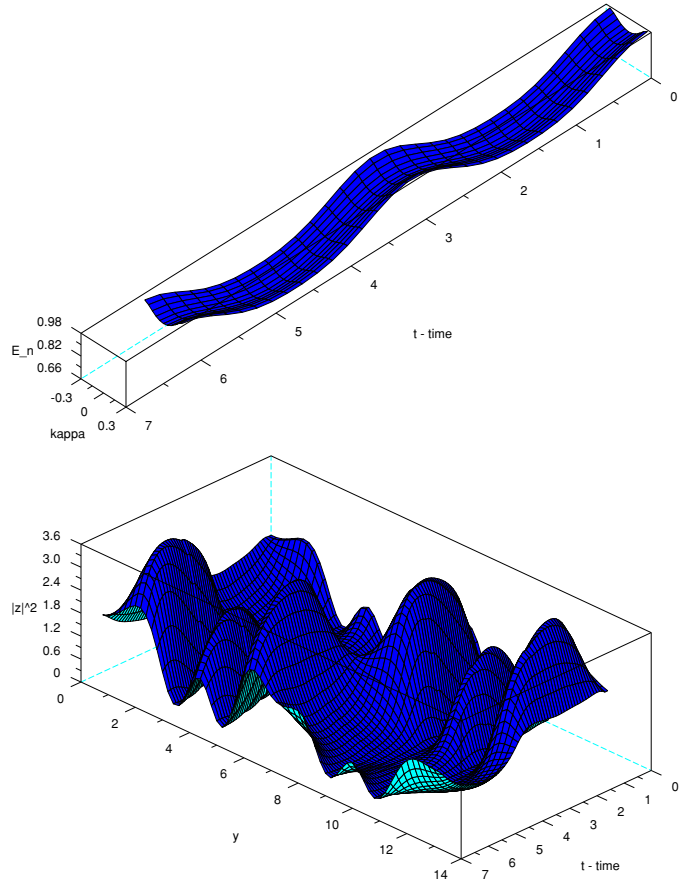

Figure 4. Time evolution of E_n (top) and $|z_{n,\kappa=0}|^2$ (bottom) for (15).

4.1. One wavenumber

We first consider the perturbed potential which is 4π-periodic:

$$\tilde{V}_{\text{per}}(t, y) = \cos\left(y - \frac{\pi}{6}\sin(ky - t)\right), \qquad \omega = k = \frac{1}{2}. \tag{15}$$

The corresponding Brillouin zone is therefore $\tilde{\mathcal{B}} = \left[-\frac{1}{4}, \frac{1}{4}\right]$ and figure 4 displays both the first conduction band and its associated modulation $|z_{n,\kappa=0}|^2$. The n index corresponds to the first conduction band, namely the first one with positive effective mass lying partially above the potential well. As time t goes by, the band is slightly deformed and not just translated. The initial data are of the form (10) with $\varphi(t = 0, x) = \cos(x - \pi)/10$ and $|a_0|^2(t = 0, x) = \exp(-(x - \pi)^2)/\pi$. We iterated up to $T = 5$ and the comparison between position densities is shown in figure 5 for $\varepsilon = 1/35$. The agreement is very satisfying and one even observes the weak convergence as ε decreases from $1/5$ to $1/35$ by checking the L^1 norm of (14). The following perturbed potential is still 4π-periodic, but slightly more involved,

$$\tilde{V}_{\text{per}}(t, y) = \cos\left(y - \frac{\pi}{6}(0.7\sin(ky - t) + 0.3\cos(ky - t))\right), \tag{16}$$

where $\omega = k = \frac{1}{2}$. Results in $T = 5$ are shown in figure 6; once again, the agreement between both computations can be considered satisfying especially for $\varepsilon = 1/47$.

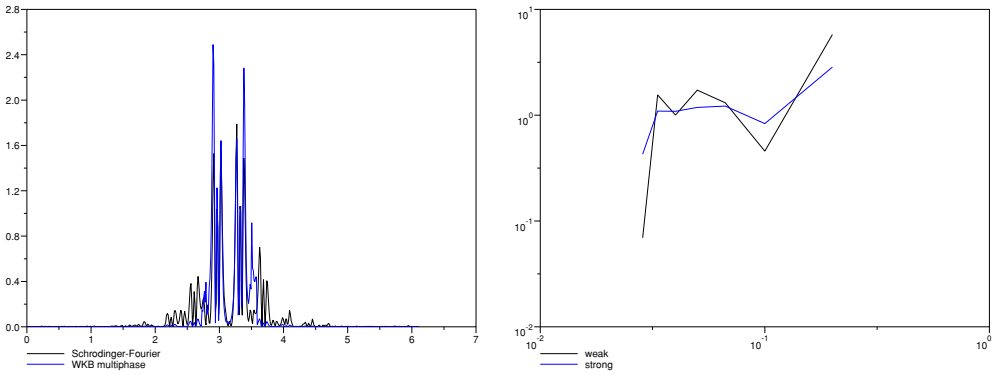

Figure 5. Position density for (15) in $T = 5$ and $\varepsilon = 1/35$ (left) and weak convergence as $\varepsilon \to 0$ ($L^1(\mathbb{R})$ norm of (14)).

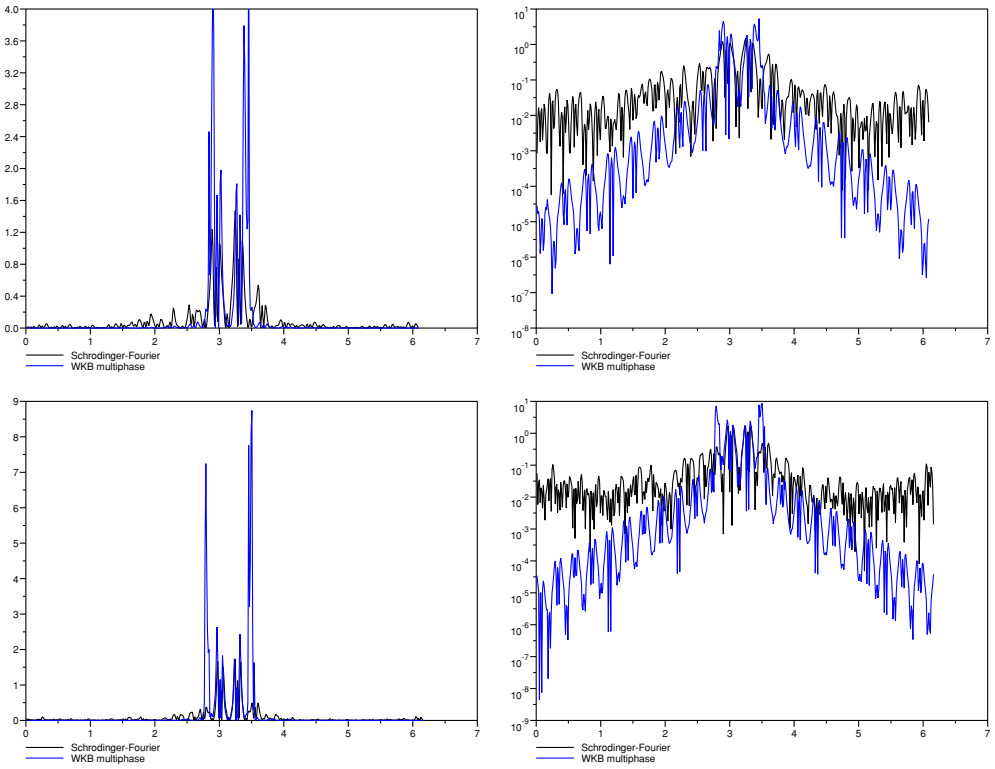

Figure 6. Position density for (16) in $T = 5$ and $\varepsilon = 1/35$ (top) and $\varepsilon = 1/47$ (bottom). Figures on the right are in log-scale.

4.2. Two different wavenumbers

We switch to the perturbed potential which is 12π-periodic:

$$\tilde{V}_{\text{per}}(t, y) = \cos\left(y - \frac{\pi}{10}(\sin(y/2 - t) + \sin(y/6 - \Omega(1/6)t))\right). \tag{17}$$

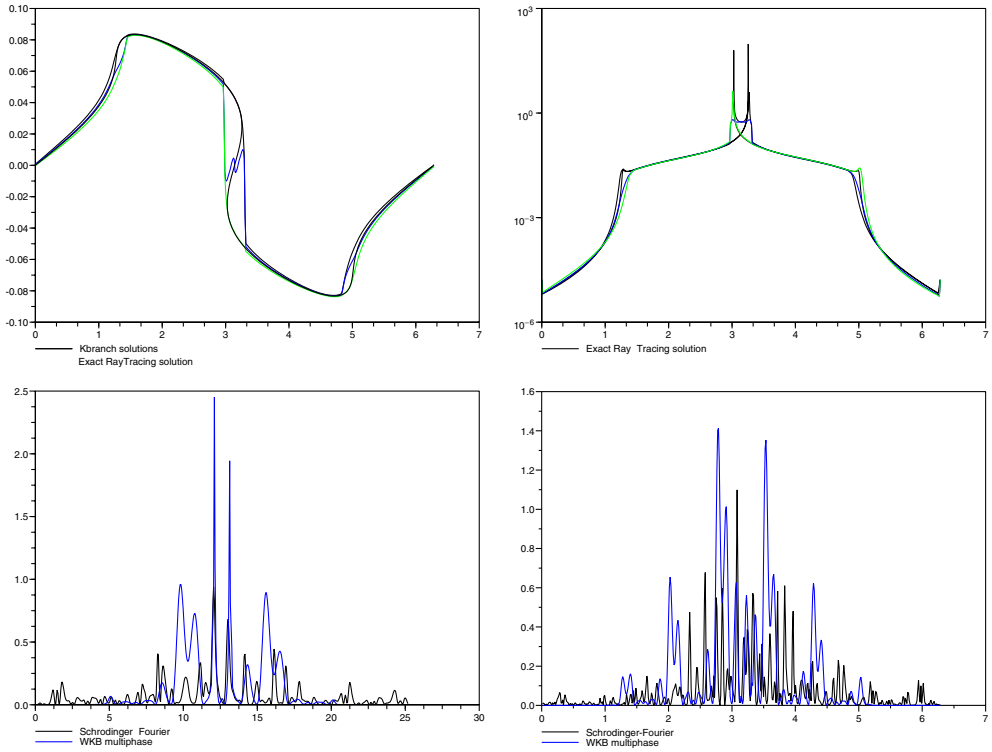

Figure 7. Three-branch velocity and intensity for (17) in $T = 30$ (top) and corresponding position density for $\varepsilon = 1/26$, $\varepsilon = 1/50$ (bottom).

This case is difficult because the Brillouin zone is very small ($k_1 = \frac{1}{6}$ and $k_2 = \frac{1}{2}$); thus (by smoothness) the bands are nearly flat and one must iterate for a long time to observe the dynamics. Figure 7 displays the outcome in $T = 30$ of both WKB approach and direct Schrödinger computations from the initial data (10) with $\varphi(t = 0, x) = \cos(x - \pi)/12$ and $|a_0|^2(t = 0, x) = \exp(-(x - \pi)^2)/\pi$. We chose the two vibration modes $k = \frac{1}{2}$ and $k = \frac{1}{6}$ because the resulting $\tilde{V}_{\text{per}}$ is still a periodic function in y and t. Periodicity in t is important if one does not want to store all values of E_n involved in the computation. The agreement between position densities is less clear in this case; however, the two central spikes are correctly located. Three-branch solutions are very good approximations of the ray-tracing picture, see again figure 7.

4.3. Inclusion of the Poisson potential

We move back to the simple perturbed potential (15) but we include now repulsive self-interaction effects between electrons. That is to say, we add a term $V_P(t, x)\psi$ on the right-hand side of (4), where $-\partial_{xx} V_P = |\psi|^2$. As a consequence, it has not been possible to obtain a breakup and multivalued K-branch solutions for $K > 1$. The perturbed potential and the initial data are the same as in section 4.1 but iterations went only up to $T = 3$. It was not possible to display a ray-tracing solution in this weakly nonlinear case, thus we just observe a quite good equivalence between position densities in figure 8. The $L^1(\mathbb{R})$ norm of (14) decreases slowly indeed with $\varepsilon \to 0$, as shown in figure 9, whereas strong L^1 convergence does not seem to be visible.

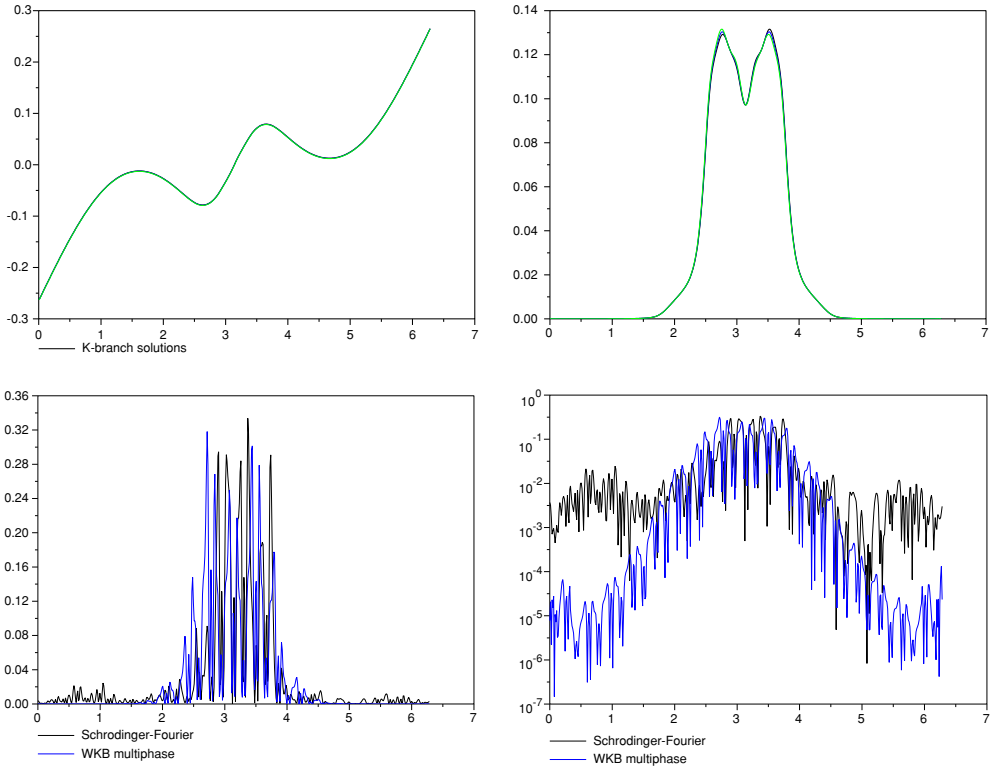

Figure 8. Three-branch velocity and intensity for (17) in $T = 3$ (top) and corresponding position density for $\varepsilon = 1/35$ (bottom).

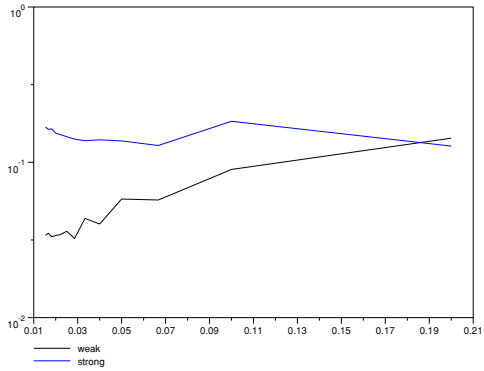

Figure 9. Decay of the $L^1(\mathbb{R})$ norm of (14) for $\varepsilon \in [1/65, 1/5]$.

5. Conclusion

We have proposed an original two-scale WKB technique adapted to electronic conduction in 1D harmonic crystals, see (7)–(10). A numerical processing has been presented together with a validation against direct Schrödinger computations. The main shortcoming in this general approach is that in case $\tilde{\mathcal{B}}$ becomes really small (that is to say, many small wavenumbers are

present in (2)), band gaps are likely to shrink so much as to allow electrons to perform interband transitions rather easily, and the assumption of staying inside a given band leading to (10) is likely to fail. Still, our ansatz (10) is more precise compared to standard phonon modelling as a collision term in a kinetic equation. Indeed, one central hypothesis in this last approach is to assume that the resulting scattering effects are instantaneous; in other terms, $\varepsilon = 0$ and an adiabatic decoupling takes place. A major open problem lies in extending our analysis in section 2 to quasi-periodic potentials; this would match the so-called incommensurate quasi-crystals, [15, 20].

Acknowledgments

Partially supported by Fundacao para Ciencia e Tecnologia, POCTI-ISFL-1-209 (Centro de Matematica e Applicacoes Fundamentais). Thanks are due to Dr R Carles for insightful comments.

References

[1] Ashcroft N W and Mermin N D 1976 *Solid-State Physics* (Austin, TX: Holt, Rinehart and Winston)
[2] Bao W Z, Jin Shi and Markowich P A 2002 On time-splitting spectral approximations for the Schrödinger equation in the semiclassical regime *J. Comput. Phys.* **175** 487–524
[3] Berry M 1984 *Proc. R. Soc. Lond.* A **392** 45
[4] Brenier Y 1984 Averaged multivalued solutions for scalar conservation laws *SIAM J. Numer. Anal.* **21** 1013–37
[5] Brenier Y and Corrias L 1998 A kinetic formulation for multibranch entropy solutions of scalar conservation laws *Ann. I. H. P. Nonlinear Anal.* **15** 169–90
[6] Carles R, Markowich P and Sparber C 2004 Semiclassical asymptotics for weakly nonlinear Bloch waves *J. Stat. Phys.* **117** 343–75
[7] Dimassi M, Guillot J C and Ralston J 2002 Semiclassical asymptotics in magnetic Bloch bands *J. Phys. A: Math. Gen.* **35** 7597–605
[8] Gosse L 2002 Using k-branch entropy solutions for multivalued geometric optics computations *J. Comput. Phys.* **180** 155–82
[9] Gosse L and Markowich P A 2004 Multiphase semiclassical approximation of an electron in a one-dimensional crystalline lattice: I. Homogeneous problems *J. Comput. Phys.* **197** 387–417
[10] Gosse L 2004 Multiphase semiclassical approximation of an electron in a one-dimensional crystalline lattice: II. Impurities, confinement and Bloch oscillations *J. Comput. Phys.* **201** 344–75
[11] Gosse L and Mauser N J 2006 Multiphase semiclassical approximation of an electron in a one-dimensional crystalline lattice: III. From *ab-initio* models to WKB for Schrödinger–Poissonab-initio *J. Comput. Phys.* **211** 326–46
[12] Gosse L and Runborg O 2005 Finite moment problems and applications to multiphase computations in geometric optics *Commun. Math. Sci.* **3** 373–92
[13] Guillot J C, Ralston J and Trubowitz E 1988 Semiclassical asymptotics in solid-state physics *Commun. Math. Phys.* **116** 401–15
[14] Hövermann F, Spohn H and Teufel S 2001 Semiclassical limit for the Schrödinger equation for a short scale periodic potential *Commun. Math. Phys.* **215** 609–29
[15] de Lange C and Janssen T 1983 Electrons in incommensurate crystals: spectrum and localization *Phys. Rev.* B **28** 195–209
[16] Markowich P, Mauser N J and Poupaud F 1994 A wigner-function approach to semiclassical limits: electrons in a periodic potential *J. Math. Phys.* **35** 1066–94
[17] Mishra S and Satpathy S 2003 One-dimensional photonic crystal: the Kronig–Penney model *Phys. Rev.* B **68** 045121
[18] Nieto J 2001 A generalized mean-field approach to the polaron *Math. Models and Meth. Appl. Sci.* **11** 1597–607
[19] Niu Q 1986 Quantum adiabatic particle transport *Phys. Rev.* B **34** 5093–100
[20] Quilichini M and Janssen T 1997 Phonon excitations in quasicrystals *Rev. Mod. Phys.* **69** 277–314
[21] Runborg O 2000 Some new results in multiphase geometrical optics *Math. Mod. Numer. Anal.* **34** 1203–31
[22] Sundaram G and Niu Q 1999 Wave-packet dynamics in slowly perturbed crystals: gradient corrections and Berry-phase effects *Phys. Rev.* B **59** 14915–25